

Temporal changes in magnetic resonance imaging in the *mdx* mouse

Su Xu^{1,2}, Stephen JP Pratt³, Roger J Mullins^{1,2}, and Richard M Lovering³

¹Department of Diagnostic Radiology and Nuclear Medicine, University of Maryland School of Medicine, Baltimore, Maryland, United States, ²Core for Translational Research in Imaging @ Maryland, Baltimore, Maryland, United States, ³Department of Orthopaedics, University of Maryland School of Medicine, Baltimore, Maryland, United States

Introduction

Duchenne muscular dystrophy (DMD) is characterized clinically by severe, progressive loss of muscular function. MRI has been used to assess DMD patients¹ and *mdx* mice^{2,3}, the murine model of DMD. Much of what is known about dystrophin structure-function is derived from studies of dystrophin-deficient animals^{4, 5}, with the most common model being the *mdx* mouse. Although *mdx* mice have muscle pathology, the phenotype is much less severe than that seen with DMD. A "critical period" has been described for the *mdx* mouse⁶, wherein there is a peak in muscle weakness and degeneration/regeneration between the 2nd and 5th weeks of life. Throughout the rest of their lifespan, *mdx* mice show marked susceptibility to contraction-induced injury, but only minimal weakness, and mechanical function is much less compromised than in DMD, so that the lifespan of the *mdx* mouse is normal. A number of studies have employed small animal MRI to examine skeletal muscle in various dystrophic models^{4, 5, 7-10}. T₂ has been reported to be elevated in both human and murine forms of muscular dystrophy, but such studies represent a snapshot in time rather than a longitudinal view. In the present study, we examined MRI of dystrophic hindlimb muscles (*mdx* mouse) over time. The goal is to relate these findings to monitoring muscular dystrophy disease progression in animal models.

Materials and Methods

In vivo MRI experiments

All protocols were approved by the University of Maryland Institutional Animal Care & Use Committee. We monitored a dystrophic (*mdx*, C57BL/ScSn-DMD^{*mdx*}) male mice every 5 weeks from 5 to 80 weeks of age and compared the results to imaging in a healthy, wild type mouse.

In vivo MRI studies were performed on a Bruker Biospec 7.0 Tesla 30-cm horizontal bore scanner using Paravision 5.1 software. A Bruker four-element ¹H surface coil array was used as the receiver and a Bruker 72 mm linear-volume coil as the transmitter. Mouse was anesthetized in an animal chamber with a gas mixture of O₂ (1 L/min) and isoflurane (3%). The animal was then placed supine on a custom made body holder bed and the radio frequency coil was positioned and fixed with surgical tape in the region of interest on the animal leg. After the animal was moved into the center of the magnet, the isoflurane level was maintained at 1.0 to 1.5% for the remainder of the experiment. An MR-compatible small-animal monitoring and gating system was used to monitor animal respiration rate and body temperature. Mouse body temperature was maintained at 36 – 37 °C using a warm water circulator.

Three-slice (axial, mid-sagittal, and coronal) scout rapid acquisition with fast low angle shot MR imaging (FLASH) was used to localize the leg. High resolution T₂-weighted MRI images in the cross-sectional view between the knee and the ankle were acquired using rapid acquisition with relaxation enhancement (RARE) sequence with TR/TE = 5000/32 ms, RARE factor = 8, field of view (FOV) = 30 x 30 mm², matrix size = 250 x 250, slice thickness = 0.5 mm without a gap, averages = 16, number of slice = 32.

Image Processing

The high resolution cross-sectional T₂-weighted images were processed using the coherence-enhancing diffusion, segmentation and histogram functions of MIPAV with a semi-auto "live-wire" tracing tool in order to separate the high signal intensity regions inside of muscle from the rest of the muscle tissue in the view. Five consecutive MRI slices without a gap which were centered on the triangle shaped tibia (Fig.2) in the thickness at 0.5 mm were used for image volume quantification.

Results

Images of healthy wild type muscles are homogeneous at 7 T (Fig 1A). By contrast, the images of *mdx* muscles are heterogeneous with multiple, unevenly distributed focal hyperintensities throughout the bulk of the muscles (Fig 1B and Fig 2). Interestingly, the heterogeneity in *mdx* muscles does not appear to be a fixed, permanent condition, but instead changes over time. The data from the 14 different time points from the *mdx* mouse showed these same unevenly distributed focal hyperintensities with a peak occurring just after the critical period (Fig 3).

Discussions and Conclusions

In the present study, we performed *in vivo* MRI to examine differences in *mdx* muscles over time. The data clearly shows areas of brightness in *mdx* muscles, which peaks near the critical period, when the muscle are thought to undergo maximal degeneration/regeneration. Such findings suggest that researchers need to consider the age of *mdx* mice when evaluating MRI findings.

McIntosh et al² provided one of the first studies to use MRI to assess skeletal muscle in *mdx* mice. In that study, the authors noted heterogeneous signal intensity on T₂-weighted images is typically noted in *mdx* hindlimb muscles; such foci of high intensity have also been noted by others^{3, 10}. In DMD, there is a progressive replacement of skeletal muscle by fatty tissue with disease progression, but it is now clear that the heterogeneity in the T₂ signal in *mdx* mice is not due to fatty infiltrate^{10, 11}. This is likely due to the fact that the severity of pathology in *mdx* does not match that of DMD.

We know a great deal about the genetic basis of muscular dystrophies, and the molecular advances have greatly improved diagnostic capabilities. However, the pathophysiology of muscle injury in normal and dystrophic skeletal muscles remains unclear. The impact of these findings will be of value in monitoring muscular dystrophy disease progression in animal models and could be useful in following the course of chronic muscle diseases in humans.

References

1. Finanger et al. *Phys Med Rehabil Clin N Am* 23: 1-10, ix, 2012.
2. McIntosh et al. *Biochem Cell Biol* 76: 532-541, 1998.
3. McMillan et al. *J Biomed Biotechnol* article ID 970726, 2011.
4. Schmidt et al. *Radiology* 250: 87-94, 2009.
5. Straub et al. *Magn Reson Med* 44: 655-659, 2000.
6. Chamberlain et al. *FASEB J* 21: 2195-2204, 2007.
7. Amthor et al. *Neuromuscul Disord* 14: 791-796, 2004.
8. Dunn et al. *Muscle Nerve* 22: 1367-1371, 1999.
9. Tardif-de et al. *Neuromuscul Disord* 10: 507-513, 2000.
10. Walter et al. *Magn Reson Med* 54: 1369-1376, 2005.
11. Xu et al. *J Appl Physiol* 2012.

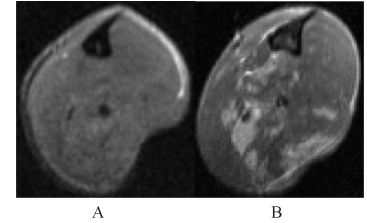


Fig 1. *In vivo* T₂-weighted MR images of the hindlimb muscle centered on the triangle shaped tibia in a cross view from both WT (A) and *mdx* (B) mice

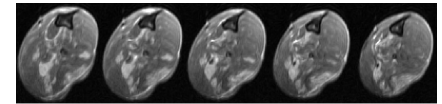


Fig 2. Five consecutive MR T₂-weighted images of an *mdx* mouse in the cross view

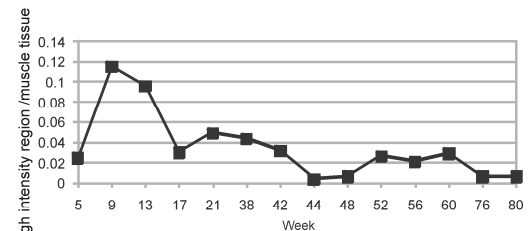


Fig 3. Temporal changes in the MRI signal distribution in the hindlimb muscle of an *mdx* mouse